

# Full-wave method of calculation of electromagnetic fields in stratified media

N. G. Lehtinen<sup>1</sup>

T. F. Bell<sup>2</sup>

U. S. Inan<sup>3</sup>

**Abstract** – Stanford Full Wave Method (SFWM) is capable of calculating monochromatic electromagnetic waves in an arbitrary stationary anisotropic plane-stratified medium with arbitrary dielectric permittivity and magnetic permeability tensors, given in each layer of the medium. The electromagnetic radiation may be emitted by an arbitrary configuration of harmonically varying currents (both electric and magnetic). The typical problems to which SFWM has been applied are: (1) transport of plane waves upward through the ionosphere and their attenuation; (2) radiation from ionosphere regions, such as electrojet currents modulated by HF heating; (3) radiation from ground-based transmitters; (4) radiation from lightning; (5) Earth-ionosphere waveguide modes; (6) scattering on ionospheric disturbances.

## 1 INTRODUCTION

There is a plethora of methods for finding fields in stratified media, which are summarized, e.g., by [1], chapter 18. However, many of them have difficulty with numerical stability when the evanescent wave solutions (with a large imaginary component of the vertical wave number) “swamp” the waves of interest, which requires special measures to contain the stability, such as subtraction of the swamping mode [2]. A detailed discussion of this effect can be found in [1, p.574-576]. Here we describe a method which is inherently stable against such “swamping.” It is based on the idea of recursive calculation of reflection coefficients and mode amplitudes by [3] and also allows the use of an arbitrary configuration of the radiating sources.

## 2 DESCRIPTION OF THE ALGORITHM

In this Section, we analyze the recently developed [4] SFWM algorithm by describing the procedure of calculation of the electromagnetic field in free space and with current sources, and the choice of optimal grid in transverse wave-vector space.

### 2.1 Waves in free space

SFWM takes advantage of the conservation of the transverse wave vector component  $\mathbf{k}_\perp$  (Snell's law). In each layer and for a given  $\mathbf{k}_\perp$  we solve the Booker equation to find four different vertical wavenumbers  $k_z$  and the corresponding four modes. We split them into two upward and two downward modes, according to the value of the imaginary component of  $k_z$ , so that the waves attenuate in the direction of their propagation. The upward and downward wave amplitudes form vectors of length two,  $\mathbf{u}$  and  $\mathbf{d}$ , respectively. The reflection coefficients  $R^u$  and  $R^d$  are  $2 \times 2$  matrices which convert upward and downward waves into each other. E.g., above the sources  $\mathbf{d} = R^u \mathbf{u}$ , while below the sources  $\mathbf{u} = R^d \mathbf{d}$ . The reflection coefficient from above,  $R^u$ , is calculated starting at the upper boundary of the system (if the free boundary is assumed, there we have  $R^u = 0$ ) and recursively going through layers downwards. The upward amplitude  $\mathbf{u}$  is calculated starting at the lower boundary of the system and recursively going upwards. Traversing the boundaries between layers is done using the continuity of horizontal components of electric and magnetic fields  $\mathbf{E}_\perp$  and  $\mathbf{H}_\perp$ . For  $R^d$  and  $\mathbf{d}$ , the direction of recursion is opposite. This direction of recursion ensures that SFWM is stable against the “swamping” instability by evanescent waves, which is a problem for many similar methods.

Independent calculation of waves with different  $\mathbf{k}_\perp$  allows the code to be easily parallelized. The solution consisting of partial waves in the  $\mathbf{k}_\perp$ -domain is converted to the position  $\mathbf{r}_\perp$ -space by an inverse Fourier transform, thus providing a full wave 3D solution at any point in the medium.

### 2.2 Modeling of sources

The electromagnetic radiation may be emitted by an arbitrary configuration of harmonically varying currents (both electric and magnetic), which are modeled as flowing in the boundaries between layers and are included in the method as boundary

---

<sup>1</sup> Electrical Engineering Department, Stanford University, 350 Serra Mall, Stanford, CA 94305, U.S.A., e-mail: nleht@stanford.edu, tel.: +1 808 256 1864, fax: +1 650 723 9251.

<sup>2</sup> Electrical Engineering Department, Stanford University, 350 Serra Mall, Stanford, CA 94305, U.S.A., e-mail: bell@nova.stanford.edu, tel.: +1 650 723 3587, fax: +1 650 723 9251.

<sup>3</sup> Electrical Engineering Department, Stanford University, 350 Serra Mall, Stanford, CA 94305, U.S.A.; Koç University, Rumelifeneri Yolu 34450 SARIYER, İstanbul, Turkey, e-mail: inan@stanford.edu, fax: +1 650 723 9251.

conditions on electric and magnetic fields  $\mathbf{E}_\perp$  and  $\mathbf{H}_\perp$ . Each boundary thus emits an upward wave (above the boundary)  $\mathbf{u}^+$  and downward wave (below the boundary)  $\mathbf{d}^-$  which are found from the jumps in the field  $\Delta\mathbf{E}_\perp$  and  $\Delta\mathbf{H}_\perp$  which are converted into  $\Delta\mathbf{u}=\mathbf{u}^+-\mathbf{u}^-$  and  $\Delta\mathbf{d}=\mathbf{d}^+-\mathbf{d}^-$ , with  $\mathbf{u}^\pm$  and  $\mathbf{d}^\pm$  connected by  $\mathbf{R}^{\text{u,d}}$ . The waves emitted by different boundaries are independent from each other due to linearity of the problem, and therefore are simply added together to find the total amplitudes.

### 2.3 Choice of the grid in $\mathbf{k}_\perp$ space

The inverse Fourier transform  $\mathbf{k}_\perp \rightarrow \mathbf{r}_\perp$  was initially implemented numerically [4] as a discrete transform using a uniformly spaced rectangular grid, which allowed utilization of the Fast Fourier Transform (FFT) algorithm. However, close examination indicated that this approach is not the most efficient because of the presence of resonances in  $\mathbf{k}_\perp$ . These resonances are due to reflections from the Earth surface and the lower ionospheric boundary, correspond to waveguide modes and have a narrow width which does not allow using a uniformly spaced grid without running into an aliasing problem. To properly implement the inverse Fourier transform requires integration through the resonances with desired accuracy, which was implemented in [5] by using more integration points in the vicinity of the resonance, while, to preserve computational efficiency, a sparser integration grid was used at values of  $\mathbf{k}_\perp$  far from the resonances.

## 3 APPLICATIONS OF SFWM

The often used class of applications of SFWM is ELF/VLF wave generation and propagation in the Earth's atmosphere and  $D$  and  $E$ -region ionosphere, which is modeled as a horizontally-stratified magnetized plasma, with an arbitrary direction of the geomagnetic field  $\mathbf{B}_g$ . For this class of applications, SFWM calculates both whistler waves radiated into ionosphere and ELF/VLF waves radiated into the Earth-ionosphere waveguide. The problems to which SFWM has been applied up to the present moment are: (1) transport of plane waves upward through the ionosphere and their attenuation; (2) radiation from ionosphere regions, such as electrojet currents modulated by HF heating; (3) radiation from ground-based transmitters; (4) radiation from lightning; (5) Earth-ionosphere waveguide modes; (6) scattering on ionospheric disturbances (in Born approximation).

### 3.1 Plane waves transport through ionosphere

The VLF waves traveling through ionosphere from below attenuate in the  $D$ -region and convert to whistlers in the magnetized plasma of the  $E$ - and  $F$ -

regions of the ionosphere. The attenuation in the QL (quasi-longitudinal) approximation and without taking into account the downward reflection was calculated by [6], for both daytime and nighttime ionosphere and for various geomagnetic latitudes. SFWM daytime results agree with [6], while at nighttime the reflection decreases the transferred energy appreciably (by  $\sim 4$  dB) compared to [6]. For non-zenith incidence (which is relevant, e.g., in the vicinity of a vertical dipole VLF transmitter) the transmitted energy is maximized when the ray is aligned with  $\mathbf{B}_g$ . The last case is shown in Figure 1.

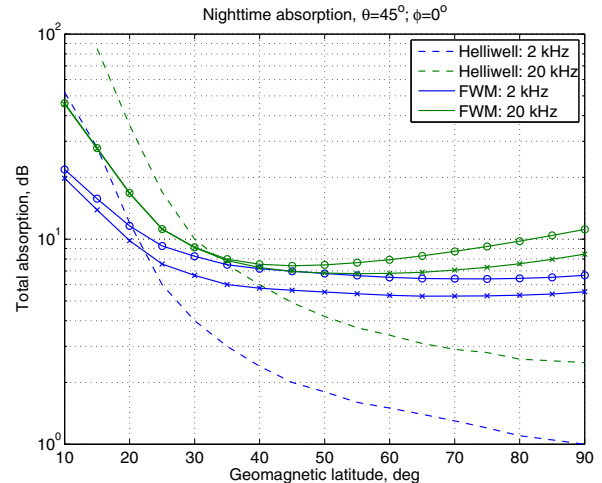


Figure 1: Total losses (including absorption and reflection) for TE (circles) and TM (crosses) modes incident at nighttime ionosphere at  $45^\circ$  with vertical in the plane of geomagnetic field.

### 3.2 Modulated electrojet current radiation

The SFWM is applied [4] to electrojet currents modulated at frequency of 1875 Hz by the HAARP HF heating facility. The change in the electrojet currents is calculated for heating of the ionosphere by a sinusoidally modulated fully-focused HF beam at 3.2 MHz and effective radiated power (ERP) of  $\sim 24$  MW. The modulated currents are horizontal, and occupy a volume which has a shape of a horizontal pancake of radius  $\sim 23$  km and thickness of  $\sim 5$  located at  $\sim 80$  km altitude. A vertical slice of two components of calculated fields is shown in Figure 2, in which the  $x$ -axis is chosen in the eastward direction, and  $y$ -axis in the northward direction. The energy emitted upward forms a relatively narrow collimated "column", with the horizontally integrated total of  $\sim 3$  W, which is inside the range 0.32–4 W previously estimated from satellite observations. The calculated magnetic field on the ground 1–2 pT is similar to the field measured at VLF sites in immediate vicinity of HAARP heating facility. The total emission into the Earth-ionosphere waveguide at horizontal distance of 50 km is calculated to be  $\sim 1$  W.

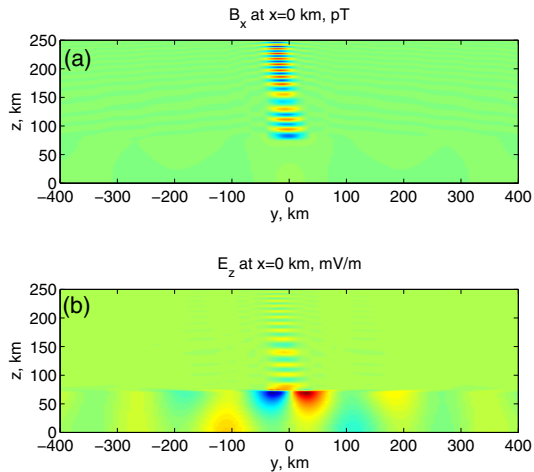


Figure 2: Fields in the  $x=0$  plane: (a)  $B_x$ ; (b)  $E_z$ . The upper panel illustrates the formation of the whistler collimated beam, and the lower panel the propagation in the Earth-ionosphere waveguide.

### 3.3 Radiation from ground-based transmitters

In Figure 3, we calculated the upward energy flux from NWC VLF transmitter, which radiates 1 MW of power at 19.8 kHz. Angle of  $\mathbf{B}_g$  with the vertical is  $35^\circ$ , which causes displacement of the pattern in the northward direction (along  $\mathbf{B}_g$ ). The concentric circles are due to mode interference. Note that beside strong North-South asymmetry, there is also pronounced East-West asymmetry (more radiation westward). In comparison with experimental data, some discrepancies were found [5] that point to existence of field-aligned irregularities in the ionosphere which attenuate and guide the VLF energy.

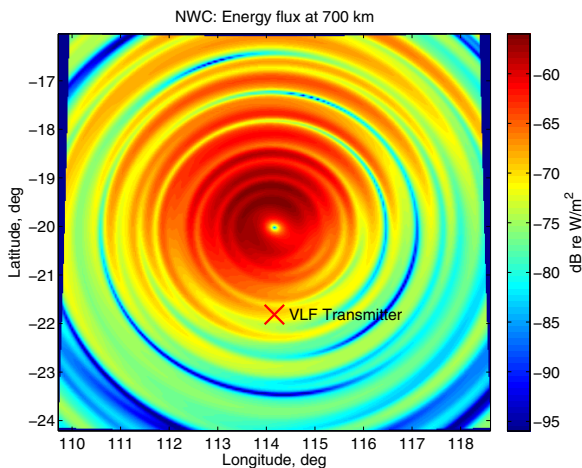


Figure 3: Upward energy flux above NWC VLF transmitter that would be seen by a satellite in an ideal stratified ionosphere.

### 3.4 Radiation from lightning

The VLF radiation from thunderstorms as seen on a satellite makes up V- and U-shaped “streak” patterns

on time-frequency spectrograms [7]. These “streaks” may be explained by interference of Earth-ionosphere waveguide modes. A similar structure is observed on the ground, by taking an inverse Fourier transform  $\omega \rightarrow t$  of which one may obtain the lightning sferic time waveforms, an example of which is shown in Figure 4.

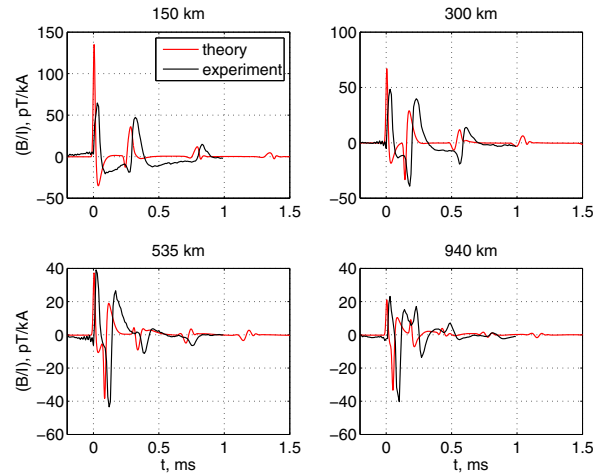


Figure 4: Calculated sferic waveforms compared to typical experimental waveforms [R. Said, personal communication].

### 3.5 Earth-ionosphere waveguide modes

The mode horizontal wavenumbers are calculated from the modal (dispersion) relation [8]

$$\det(1-R^d R^u) = 0 \quad (1)$$

where the reflection coefficients are taken at the same altitude. An example of calculated strongest emitted modes as a function of altitude is presented in Figure 5.

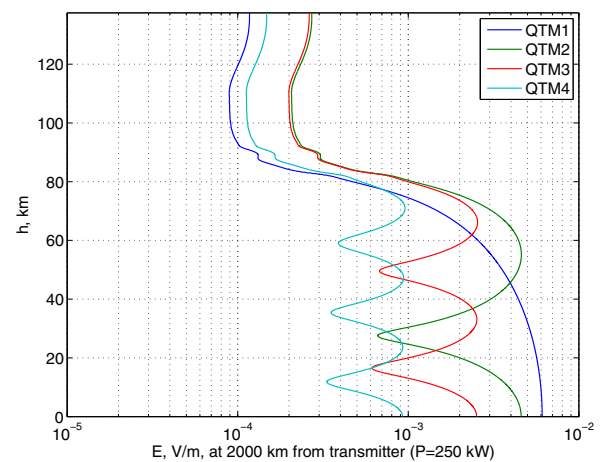


Figure 5: Calculated E field in the strongest modes emitted by NLK transmitter at the distance of 2000 km towards HAARP.

### 3.6 Scattering on ionospheric disturbances

The scattering of the VLF waves on ionospheric disturbances has been calculated using Born approximation [8]. The waves are assumed to be propagating in a stratified medium and the disturbance is included in SFWM as a source with additional currents created by the incident field acting only on the change in the conductivity. The condition for the use of this approximation is for the disturbance to be small, so that the scattered field inside the disturbance is small compared to the incident field. The change of the VLF amplitude measured on the ground is due to the scattered field and is presented in Figure 6 for a disturbance caused by a lightning EMP (electromagnetic pulse) which changes the electron density. In particular, it was found that the scattering is strongest for westward-propagating waves.

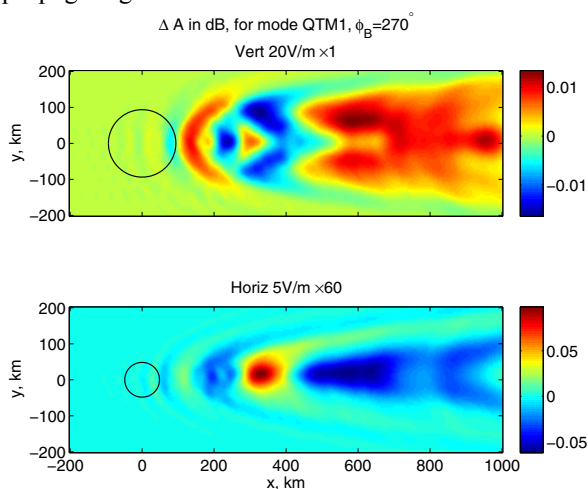


Figure 6: The VLF amplitude change  $\Delta A$  on the ground as a function of the position of the receiver, for an incident QTM1 mode in  $+x$  (westward) direction. The location of the disturbance is marked by a circle. Upper panel: Lightning EMP creates an annular disturbance (from a vertical lightning discharge). Lower panel: the disturbance is pancake-shaped (from a horizontal discharge).

#### 4 FUTURE WORK

The planned near future work on SFWM includes the following:

- more accurate calculation of scattering on strong disturbances using the method of moments approach;
- inclusion of the effects of Earth's curvature;
- introduction of the long-distance waveguide propagation capability by using a segmented path of a VLF signal.

#### 5 SUMMARY

SFWM is stable against numerical “swamping” and is easily parallelized, which makes it an extremely useful computational tool for solving various problems involving radiation and propagation of waves in stratified anisotropic media. The applications so far included VLF propagation in Earth’s lower ionosphere and atmosphere; however, the generality of the used algorithm may open possibilities of its use in other areas.

#### Acknowledgments

This work was supported by ONR grant N0014-09-1-0034, NSF grant ATM-0836326, DARPA grant HR-0011-10-1-0058, DoAF grant FA9453-11-C0011 and DTRA grant HDTRA-10-1-0115 to Stanford University.

#### References

- [1] K. G. Budden, “The propagation of radio waves: the theory of radio waves of low power in the ionosphere and magnetosphere”, Cambridge University Press, Cambridge, 1985.
- [2] M. L. V. Pitteway, “The numerical calculation of wave-fields, reflexion coefficients and polarizations for long radio waves in the lower ionosphere I”, *Phil. Trans. R. Soc. A*, 257 (1079), 219–241, 1965.
- [3] T. Nygrén, “A method of full wave analysis with improved stability”, *Planet. Space Sci.*, 30(4), 427–430, doi:10.1016/0032-0633(82)90048-4, 1982
- [4] N. G. Lehtinen and U. S. Inan, “Radiation of ELF/VLF waves by harmonically varying currents into a stratified ionosphere with application to radiation by a modulated electrojet”, *J. Geophys. Res.*, 113, A06301, doi:10.1029/2007JA012911, 2008.
- [5] Lehtinen, N. G. and U. S. Inan, “Full-wave modeling of transionospheric propagation of VLF waves”, *Geophys. Res. Lett.*, 36, L03104, doi:10.1029/2008GL036535, 2009
- [6] R. A. Helliwell, “Whistlers and related ionospheric phenomena”, Stanford Univ. Press, Stanford, 1965.
- [7] M. Parrot, U. S. Inan, and N. G. Lehtinen, “V-shaped VLF streaks recorded on DEMETER above powerful thunderstorms”, *J. Geophys. Res.*, 113, A10310, doi:10.1029/2008JA013336, 2008.
- [8] N. G. Lehtinen, R. A. Marshall, and U. S. Inan, “Full-wave modeling of “early” VLF perturbations caused by lightning electromagnetic pulses”, *J. Geophys. Res.*, 115, A00E40, doi:10.1029/2009JA014776, 2010.